Base-free, simple and scalable synthesis of new, air- and moisture-stable [Ru^{III}($PyNHC^R$)$(Cl)_3(H_2O)$] complexes as precursors for Ru(II)-PyNHC complexes

Nida Shahid, Rahul Kumar Singh, Navdeep Srivastava, Amrendra K. Singh*

A series of Ru(III)-PyNHC complexes, identified as [Ru^{III}($PyNHC^R$)$(Cl)_3(H_2O)$] (1a–c), have been prepared following a base-free route. The structurally simple, air and moisture stable complexes represent rare examples of Ru(III)-NHC complexes. Further, these benchtop stable Ru(III)-PyNHC complexes were shown to be excellent metal precursors for the synthesis of new [Ru^{II}($PyNHC^R$)$(Cl)_2(PPh_3)_2$] (2a-c) and [Ru^{II}($PyNHC^R$)(CNC^{Me})I]PF_6 (3a-c) pincer complexes. All the complexes have been characterised using spectroscopic methods, and structures of 1a, 1b, 2c and 3a have been determined using the single-crystal X-ray diffraction technique.

The chemistry of coordination and organometallic complexes of ruthenium has continued to grow at unprecedented rates in the last few decades.[1–4] Ruthenium complexes have found applications in many industrial and scientific fields such as catalysis,[5–8] solar cells,[3] material sciences[9] and medicinal chemistry.[10] Ruthenium, the cheapest noble metal combined with its diverse applications, has attracted researchers from academia and industry to develop new Ru complexes with novel or improved properties and applications. The majority of synthetic pathways for the preparation of new Ru complexes start from one of the common, stable Ru-metal precursor complexes like $Ru^{III}Cl_3 \cdot xH_2O$, [$(Cp^*Ru^{III}(Cl)_2]_2$ $Ru^{II}(Cl)_2(PPh_3)_3$, $Ru^{II}(H)_2(CO)(PPh_3)_3$, $Ru^{II}(H)(Cl)(CO)(PPh_3)_3$, $Ru^{II}(Cl)_2(DMSO)_4$, $[Ru^{II}(Cl)_2$(*p*-cymene)$]_2$, $[Ru^{II}(Cl)_2(COD)]_n$, $[Ru^{II}(Cl)_2(CO)_2]_n$, and $[(arene)Ru^{II}(Cl)_2]_2$ to name a few. These precursor complexes play a significant role in the development of new Ru complexes, and a careful selection of the suitable precursor is one of the most critical parts of any synthetic strategy.

Ru complexes with NHC ligands have become increasingly popular in recent years due to improved catalytic performance[11] and tuneable stereo-electronic properties[12,13], which help in catalyst designing.[14] These Ru-NHC complexes have found applications in homogeneous organic transformations,[15,16] olefin metathesis reactions, therapeutic drugs,[10] as well as applications in dye-sensitised solar cells (DSSCs).[17] We have recently started exploring the catalytic applications of Ru(II)-CNC (CNC = pyridine-dicarbene pincer ligands) complexes with smaller N-alkyl wingtips on carbenes[18–20]. During our investigation, we have noticed that even after a few decades of research in this field, there is no Ru metal precursor with an NHC ligand already present.

Several reports on the synthesis of Ru-NHC complexes using the Ru metal precursors ($RuCl_2(PPh_3)_3$,[21] [$RuCl_2$(p-cymene)]$_2$,[22] $[Ru(Cl)_2(CO)_2]_n$,[23] etc. are present in literature where one or more of the ligands are replaced with the in situ generated NHC ligands. However, this approach to Ru-NHC complex preparation is not generalised. Most methods have shortcomings like poor yield and undesired side products and involve using other reagents like bases for carbene generation. Further, the use of the base, a general requirement for generating NHCs from their azolium precursors, has the potential to cause unintended or undesirable outcomes.[18] Nolan and co-workers have recently developed a “weak base” route for the generation of NHC-metal complexes.[24,25] The “weak base” route has been shown to be a simple, cost-effective and environmentally benign approach which can be extended further with various metals for NHC-based complexes.

Herein, we report a “base-free” synthesis of a series of Ru(III)-PyNHC complexes [Ru^{III}($PyNHC^R$)$(Cl)_3(H_2O)$] (**1a**–**c**) {$PyNHC^R$ = 3-methyl-1-(pyridine-2-yl)imidazol-2-ylidene (**1a**), 3-isopropyl-1-(pyridine-2-yl)imidazol-2-ylidene (**1b**) and 3-methyl-1-(pyridine-2-yl)benzimidazol-2-ylidene (**1c**)} derived from pyridine functionalized N-alkylated azolium salts, and $RuCl_3 \cdot xH_2O$. Further, we have utilized these Ru(III)-PyNHC complexes as metal precursors for the synthesis of a series of the corresponding Ru(II)-PyNHC-(PPh_3) complexes (**2a**–**c**) and Ru(II)-PyNHC-CNC^{Me} ($CNC^{Me} \cdot 2HBr$ = 2,6-Bis[3-

---

Department of Chemistry, Indian Institute of Technology Indore, Indore, 453552, India. Email: aks@iiti.ac.in

Electronic Supplementary Information (ESI) available: Details on preparation, characterization of compounds, spectral data, and details of DFT calculations. CCDC 2177433-2177436. See DOI: 10.1039/x0xx00000x

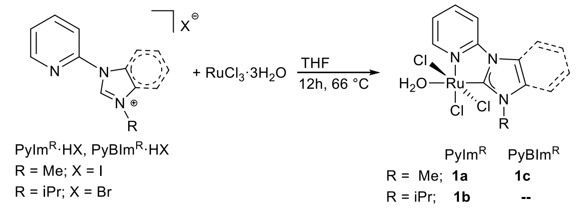

Scheme 1. Synthesis of Ru(III)-PyNHC complexes (**1a**–**c**)

(methyl)imidazolium] pyridine dibromide)pincer complexes (**3a**–**c**).

The reaction of ligand precursors with $RuCl_3\cdot3H_2O$ in 1:1 ratio in THF at reflux temperature for 12 h afforded the new Ru(III)-PyNHC complexes **1a**–**c** (Scheme 1). The synthetic route involves the Ru(III) metal centre, which is sufficiently lewis acidic in nature, for electrophilic C-H activation in pyridine functionalised azolium salts. No chemical additive, like a base, is required for the reaction. In the presence of weak or strong bases, a black powder, insoluble in water or any organic solvent, was obtained. The synthesis of **1a**–**c** has been scaled up to the gram scale starting from 1 g of $RuCl_3\cdot xH_2O$ (See SI).

The air-stable brown precipitate was filtered, washed with THF and recrystallised from MeCN or MeOH. All three complexes were obtained in good to excellent (55–85%) yields. Complexes **1a**–**c** have been characterised by IR, UV-vis spectroscopy, ESI^+-MS spectrometry, and Thermogravimetric analysis (TGA). Complexes **1a** and **1b** have also been characterised by Powder XRD, and their structures have been determined by the single-crystal X-ray diffraction technique. The paramagnetic (low spin d^5) nature of the Ru centre in these complexes was confirmed by measurement of their magnetic moment using the Evans method.[26] The values for magnetic moments were found within the range of 1.6–1.7 BM establishing the presence of one unpaired electron.

Stretching frequencies for C=N and C-C bonds obtained using IR spectroscopy were compared with the ligand precursors and found to lie within the expected range (See SI). The characteristic MLCT absorption maxima in UV-vis spectra for the Ru-NHC bond in the three complexes were observed at 387 nm (**1a**), 380 nm (**1b**) and 392 nm (**1c**). ESI^+-MS spectrograms showed peaks for the fragments $[M\text{-}Cl]^+$, $[M\text{-}Cl\text{-}H_2O]^+$, and $[M\text{-}Cl\text{-}H_2O\text{+}S]^+$ (where S=Solvent i.e., MeCN or MeOH), in complexes **1a**–**c**. HR-MS spectrogram of the molecular ion peak at m/z assignable to $[M\text{-}Cl]^+$, i.e., 348.9315 (**1a**), 376.9613 (**1b**), and 398.9501 (**1c**) confirmed the elemental composition (See SI). To determine the thermal stability of complexes (**1a**–**c**), thermogravimetric analysis was performed under a nitrogen atmosphere, which showed no weight loss in complexes up to 150 °C. TGA plots are discussed in Supplementary Information. To check the bulk purity of the sample, powder X-ray data of compounds **1a** and **1b** were compared with simulated powder XRD obtained from their single-crystal X-ray data.

Molecular structures of **1a** and **1b** were determined using single-crystal X-ray diffraction technique. Complexes **1a** and **1b** crystallised in orthorhombic (*Pna2₁*) and monoclinic (*I12/a1*) crystal systems respectively. The structures exhibited a pseudo-octahedral geometry around the Ru(III) center. The bidentate ligand formed a five membered metallacycle with a bite angle of 79.7(7)° and 78.34(19)° in **1a** and **1b** respectively. In both the structures, the coordinated H_2O ligand was replaced by solvent of crystallisation i.e., MeCN in **1a** and MeOH in **1b**. Therefore, the structure obtained for complex **1a** is denoted as **1a-MeCN**, and that of **1b** as **1b-MeOH**. Acetonitrile was observed trans to pyridine N-atom in **1a-MeCN** whereas in **1b-MeOH**, π-donor methanol was found trans to the NHC. DFT calculations of isomeric cis/trans forms w.r.t position of solvent molecule from pyridine N-atom, confirms that in case of π-acid ligand MeCN, isomer with the solvent trans to pyridine was found to be thermodynamically stable while in case of π-donor ligand the solvent molecule trans to NHC was more stable (Fig.2). In another complex Ru(II)-NO {[($PyNHC^{t\text{-}Bu}$)Ru(Cl)$_3$NO]}[27] reported earlier, the π-acid ligand NO has also been found trans to the

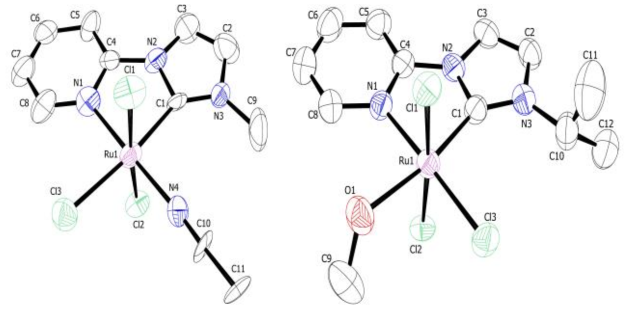

Fig. 1. ORTEP diagrams for complexes **1a-MeCN** (left) and **1b-MeOH** (right) obtained from X-ray diffraction. Hydrogen atoms and solvent molecules are excluded for clarity. Ellipsoids are shown at the 50% probability level. Selected Ru1-C1 bond distances(Å) in **1a-MeCN** and **1b-MeOH** are 2.052(16) and 2.007(5), whereas Cl1-Ru-Cl2 bond angles are 93.1(3)° and 91.2(11)° respectively.

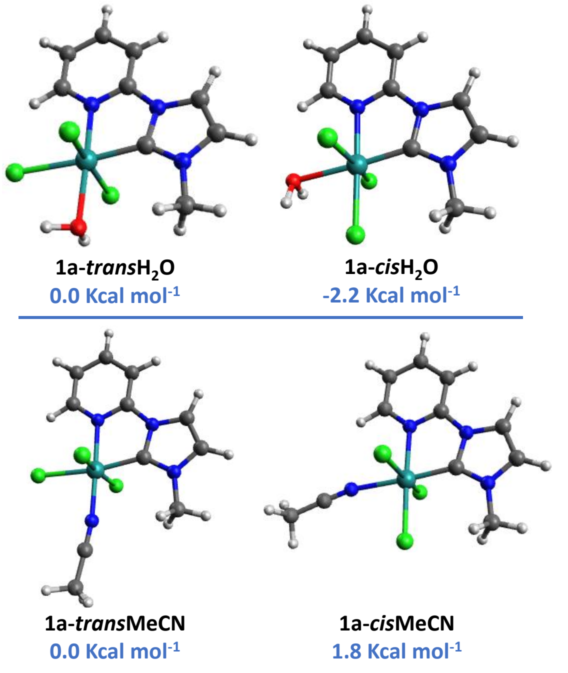

Fig.2. Optimized cis/trans isomeric forms of **1a** w.r.t solvent molecule (H_2O and MeCN) and relative Gibbs free energies (at 298.15 K) and 1M solution.

pyridine N-atom. The Ru-C$_{carbene}$ bond distance in **1b-MeOH** is shorter than the corresponding distance in **1a-MeCN** (2.052(16)Å) or the Ru(II)-NO (2.049(5) Å) reported earlier. The shortening of bond length in **1b-MeOH** could be due to the increased π-back donation from the Ru(III) centre with a π-donor MeOH ligand at the trans position. Similarly, the Ru-N$_{py}$ distance in **1b-MeOH** (2.089(4) Å) is slightly shorter than 2.10(4) Å observed in both **1a-MeCN** and Ru(II)-NO complexes. Selected bond parameters have been listed in Table S2 (see SI).

Complexes **1a-c** represent easily accessible Ru(III)-PyNHC complexes with a well-defined composition compared to $RuCl_3 \cdot xH_2O$. These complexes have been found to be air and moisture stable and can be stored at benchtop for several months with no sign of decay. Further, these complexes enrich the list of very rare Ru(III)-NHC complexes,[28–30] which have, so far, been obtained by oxidising a Ru(II)-NHC complex or Ru(II) precursor.[21] To check their usefulness as starting material for the preparation of Ru(II)-PyNHC complexes with various ancillary ligands, complexes **1a-c** have been used to prepare the phosphine complexes **2a-c** (analogous to $RuCl_2(PPh_3)_3$). Further, to demonstrate the thermal stability of these complexes as metal precursors, Ru-PyNHC-CNC pincer complexes **3a-c** have been prepared under ethylene glycol reflux conditions (~200 °C).

The reaction of complexes **1a**–**c** with a 6-fold excess of triphenylphosphine in methanol at reflux temperature gave the corresponding Ru(II)-PyNHC-(PPh$_3$) complexes formulated as $[Ru^{II}(PyNHC^R)(Cl)_2(PPh_3)_2]$ **2a**–**c** in 60–80% yield (Scheme 2). The air-stable, yellow complexes were characterised by ESI$^+$-MS, ^{1}H and ^{31}P NMR, and the molecular structure of **2c** was determined by SC-XRD techniques. HR-MS spectrogram exhibited a molecular ion peak at m/z fragment 820.1361 (**2a**), 848.1688 (**2b**), and 870.1545 (**2c**) assignable to [M-Cl]$^+$.

The poor solubility (as well as phosphine dissociation in solution) of **2a**-**c** in common organic solvents makes it difficult to obtain good quality ^{1}H NMR data. However, for **2b** in CD_3CN and **2c** in DMSO-d$_6$, ^{1}H NMR could be obtained with sufficient S/N ratio for the identification of relevant peaks. Compound **2a** was not soluble in CD_3CN, and PPh$_3$ dissociation in DMSO-d$_6$ complicated its ^{1}H NMR characterisation. The ^{31}P NMR spectra of complexes **2a** and **2c** in DMSO-d$_6$ indicate significant phosphine dissociation in solution; however, for **2b** in CD_3CN, phosphine dissociation was less prominent. The ^{31}P NMR spectra of complexes **2a** and **2c** displayed two singlets at 35.4 (**2a-PPh$_3$**), 33.3 (**2c-PPh$_3$**) and 26.8 (**2a**), 24.1 ppm (**2c**) as well as signal for free PPh$_3$ at -6.0 ppm in DMSO-d$_6$. In comparison, complex **2b** showed a singlet at 25.9 ppm in CD_3CN with less prominent peaks for PPh$_3$ dissociation.

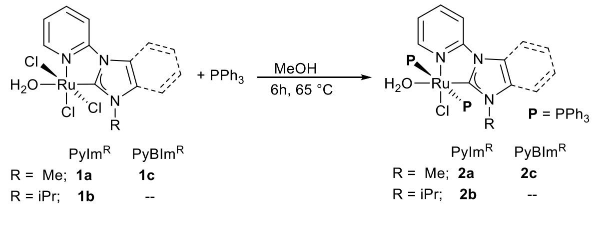

Scheme 2. Synthesis of Ru(II)-PyNHC-(PPh$_3$) (**2a**–**c**) from Ru(III)-PyNHC complexes (**1a**–**c**)

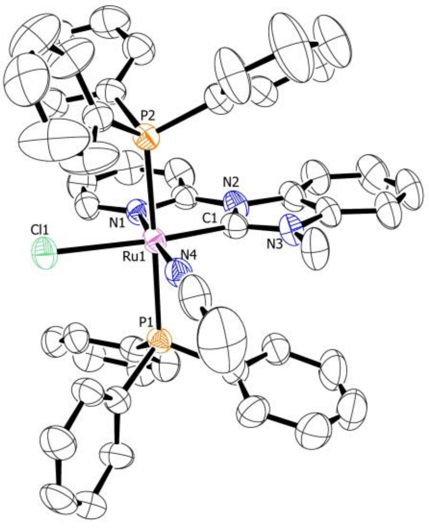

Fig. 3. ORTEP diagram of complex **2c-MeCN** obtained from X-ray diffraction. Hydrogen atoms and solvent molecules and one Cl$^-$ anion present in lattice are excluded for clarity. Ellipsoids are shown at the 50% probability level. Selected bond distances(Å) and bond angles(º) are Ru1-C1 1.965(4), Ru1-P1 2.3978(11), Ru1-P2 2.4290(12), Ru1-Cl1 2.5005(11), Ru-N1 2.088(4), Ru1-N4 2.067(4), P1-Ru1-P2 178.08(4), and N1-Ru1-N4 175.65(14).

The structure of complex **2c** was determined by X-ray crystallography (Fig. 3). It crystallised in a monoclinic (*P*2$_1$/*c*) space group and displayed a pseudo-octahedral geometry around the Ru(II) centre with a solvent (CH_3CN) bound to the metal and a Cl$^-$ counterion in the lattice (hence denoted as **2c-MeCN**). The Ru1-C1 bond length in **2c-MeCN** is 1.964(4) Å, whereas in Ru(III)-PyNHC analogues, the values for these bond distances in **1a-MeCN** and **1b-MeOH** are 2.052(16) Å and 2.007(5) Å respectively. The shorter Ru-C$_{carbene}$ bond in **2c-MeCN** can be attributed to increased π-back-donation from the Ru(II) compared to Ru(III) metal centre. In an example reported by Siemeling et al.,[21] the lengthening of bond distance was also observed upon oxidation from Ru(II)-NHC (1.972(2) Å) to Ru(III)-NHC (2.032(8) Å). Other relevant bond parameters are listed in Table S2 (see SI).

In another example for the preparation of derivatives of **1a**–**c,** we have synthesised a series of $[Ru^{II}(PyNHC^R)(CNC^{Me})I]PF_6$ pincer complexes **3a**–**c** starting from **1a-c** (Scheme 3). This approach involves the reaction of CNC pincer ligand precursor with our precursor complexes **1a**–**c** in ethylene glycol at reflux temperature (190 °C) to yield complexes **3a**–**c**. The successful synthesis of **3a**–**c** indicates the thermal stability of Ru(III)-PyNHC precursors **1a**–**c**. NaI was added to reduce the possibility of mixed halide complexes. Complexes **3a**–**c** were characterised by ESI$^+$-MS spectrometry and multinuclear NMR spectroscopy. HR-MS spectrogram exhibited a molecular ion peak at m/z fragment 627.0079 (**3a**), 655.0365 (**3b**), and 627.0242 (**3c**) assignable to [M-PF$_6$]$^+$.

The ^{1}H and ^{13}C NMR spectra of complexes **3a**–**c**, in DMSO-d$_6$, show two distinct set of signals, indicating the existence of

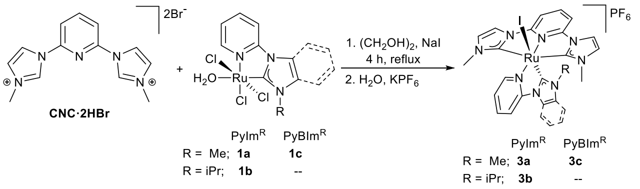

Scheme 3. Synthesis of Ru(II)-PyNHC-CNC^{Me} pincer complexes (**3a**–**c**) from Ru(III)-PyNHC complexes (**1a**–**c**)

two isomeric structures. In ^{1}H NMR, in addition to the expected, downfield shifted signal (δ 10.27 (**3a**), 10.29 (**3b**), and 10.44 ppm (**3c**) doublet) for the proton at the ortho position of the pyridine unit in the bidentate ligand PyNHC^R , another doublet at δ 9.81 (**3a**), 9.81 (**3b**) and 9.90 ppm (**3c**) is also obtained. Similarly, in the alkyl region, two sets of peaks, double the number of expected signals, are obtained. This could be due to cis/trans-isomers with respect to the two pyridine units, as has been reported earlier for structurally similar Ru-tpy complexes (tpy = terpyridine).[31] Another possibility for the existence of two signals could arise due to iodide substitution by a dmso-d$_6$ molecule resulting in an equilibrium between iodide coordinated and dissociated forms. Therefore, the trans-isomer or the iodide coordinated form show a downfield shifted signal, but the cis-isomer or the iodide dissociated form do not show such a shift. The ^{13}C NMR spectra also show two sets of peaks for the two types of carbene for CNC^{Me} ligand and the bidentate (PyNHC^R) ligand. The exact reason, out of the two possibilities, for the existence of two sets of peaks is uncertain at this time and is currently being investigated.

The solid-state structure and geometry around the Ru centre in **3a** has been confirmed by the single-crystal X-ray diffraction technique (See Supplementary Information, Fig. S38). The bond parameters cannot be reliably discussed due to poor diffraction data and low bond precision and will be included in a follow-up paper. However, the crystal structure of **3a** shows an octahedral geometry around the Ru(II) centre and confirms the structure as depicted in Scheme 3.

In summary, we report a new series of three robust, scalable, and benchtop stable Ru(III)-PyNHC complexes (**1a**–**c**) based on a (PyNHC^R) ligand frameworks bearing R = Me, and ^{i}Pr alkyl wingtips. These Ru(III) complexes with a bidentate chelating ligand containing pyridine and N-heterocyclic carbene units serve as metal precursors for the preparation of a series of Ru(II)-NHC-(PPh$_3$) (**2a**–**c**) and Ru(II)-PyNHC-(CNC^{Me}) (**3a**–**c**) complexes. The synthesis of complexes **3a-c** indicates the thermal stability as well as the usability of complexes **1a-c** in harsh reaction conditions. All new compounds have been characterised by usual characterisation techniques, and the structures of **1a**, **1b**, **2c**, and **3a** have been confirmed by SC-XRD technique. The results reported here present a straightforward route to prepare Ru(III)-PyNHC complexes from simple starting materials. Further studies on the synthesis of analogues Ru(III)-PyNHC complexes with different alkyl wingtips of the NHC units, variation of azole rings and their use as metal precursors for the synthesis of Ru(II)-NHC complexes with different ancillary ligands are currently undergoing.

This research was supported by Science and Engineering Research Board, Government of India (EMR/2016/004076) grant to AKS. RKS acknowledges CSIR, New Delhi and both NS acknowledge IIT Indore for fellowship. Authors gratefully acknowledge SIC, IIT Indore and DST-FIST 500MHz NMR Facility, Department of Chemistry, IIT Indore for characterisation data.

Notes and references

1. T. Ishizuka, H. Sugimoto, S. Itoh and T. Kojima, *Coordination Chemistry Reviews*, 2022, **466**, 214536.
2. A. Ghaderian, S. Kazim, M. Khaja Nazeeruddin and S. Ahmad, *Coordination Chemistry Reviews*, 2022, **450**, 214256.
3. L. Mauri, A. Colombo, C. Dragonetti, D. Roberto and F. Fagnani, *Molecules*, 2021, **26**, 7638.
4. A. Udvardy, F. Joó and Á. Kathó, *Coordination Chemistry Reviews*, 2021, **438**, 213871.
5. P. Nareddy, F. Jordan and M. Szostak, *ACS Catal.*, 2017, **7**, 5721–5745.
6. J. Pospech, I. Fleischer, R. Franke, S. Buchholz and M. Beller, *Angewandte Chemie International Edition*, 2013, **52**, 2852–2872.
7. C. K. Prier, D. A. Rankic and D. W. C. MacMillan, *Chem. Rev.*, 2013, **113**, 5322–5363.
8. A. Kajetanowicz and K. Grela, *Angewandte Chemie International Edition*, 2021, **60**, 13738–13756.
9. M. R. Axet and K. Philippot, *Chem. Rev.*, 2020, **120**, 1085–1145.
10. S. Thota, D. A. Rodrigues, D. C. Crans and E. J. Barreiro, *J. Med. Chem.*, 2018, **61**, 5805–5821.
11. C. W. Bielawski, D. Benitez and R. H. Grubbs, *Science*, 2002, **297**, 2041–2044.
12. E. Peris, *Chem. Rev.*, 2018, **118**, 9988–10031.
13. O. Schuster, L. Yang, H. G. Raubenheimer and M. Albrecht, *Chem. Rev.*, 2009, **109**, 3445–3478.
14. J. DePasquale, M. Kumar, M. Zeller and E. T. Papish, *Organometallics*, 2013, **32**, 966–979.
15. Q. Zhao, G. Meng, S. P. Nolan and M. Szostak, *Chem. Rev.*, 2020, **120**, 1981–2048.
16. Z.-Q. Wang, X.-S. Tang, Z.-Q. Yang, B.-Y. Yu, H.-J. Wang, W. Sang, Y. Yuan, C. Chen and F. Verpoort, *Chem. Commun.*, 2019, **55**, 8591–8594.
17. S. Aghazada, I. Zimmermann, V. Scutelnic and M. K. Nazeeruddin, *Organometallics*, 2017, **36**, 2397–2403.
18. D. Yadav, S. Misra, D. Kumar, S. Singh and A. K. Singh, *Appl Organomet Chem*, , DOI:10.1002/aoc.6287.
19. D. Yadav, R. K. Singh, S. Singh, P. M. Shirage and A. K. Singh, *Journal of Organometallic Chemistry*, 2021, **953**, 122061.
20. D. Yadav, R. K. Singh, S. Misra and A. K. Singh, *Applied Organometallic Chemistry*, **n/a**, e6756.
21. S. Hitzel, C. Färber, C. Bruhn and U. Siemeling, *Organometallics*, 2014, **33**, 425–428.
22. X. Ma, S. G. Guillet, Y. Liu, C. S. J. Cazin and S. P. Nolan, *Dalton Trans.*, 2021, **50**, 13012–13019.
23. T. Lübbering, P. D. Dutschke, A. Hepp and F. E. Hahn, *Organometallics*, 2021, **40**, 3775–3784.
24. E. A. Martynova, N. V. Tzouras, G. Pisanò, C. S. J. Cazin and S. P. Nolan, *Chem. Commun.*, 2021, **57**, 3836–3856.
25. A. Collado, J. Bohnenberger, M. Oliva-Madrid, P. Nun, D. B. Cordes, A. M. Z. Slawin and S. P. Nolan, *Eur. J. Inorg. Chem.*, 2016, **2016**, 4111–4122.
26. D. F. Evans, *J. Chem. Soc.*, 1959, 2003–2005.
27. G. F. Caramori, A. O. Ortolan, R. L. T. Parreira and E. H. da Silva, *Journal of Organometallic Chemistry*, 2015, **799–800**, 54–60.
28. P. L. Arnold and A. C. Scarisbrick, *Organometallics*, 2004, **23**, 2519–2521.
29. F. Chen, G.-F. Wang, Y.-Z. Li, X.-T. Chen and Z.-L. Xue, *Inorganic Chemistry Communications*, 2012, **21**, 88–91.
30. Y. Shimoyama, T. Ishizuka, H. Kotani, Y. Shiota, K. Yoshizawa, K. Mieda, T. Ogura, T. Okajima, S. Nozawa and T. Kojima, *Angew. Chem.*, 2016, **128**, 14247–14251.
31. H.-W. Tseng, R. Zong, J. T. Muckerman and R. Thummel, *Inorg. Chem.*, 2008, **47**, 11763–11773.